Identification of Mass-Spring-Dashpot Systems using Multiple-Model Adaptive Estimation (MMAE) Algorithms

Sajjad Fekri Asl, Michael Athans, Antonio Pascoal
Instituto Sistemas e Robótica, Instituto Superior Técnico, Lisboa 1049–001, Portugal
Email: {sfekri, athans, antonio}@isr.ist.utl.pt
Telephone: (+351) 21–8418054
Fax: (+351) 21–8418090

***Abstract*— In this paper, the performance evaluation of two configurations of the Multiple-Model Adaptive Estimation (MMAE) algorithm is shown for identification and modeling of a complex Mass-Spring-Dashpot (MSD) system. The algorithms compare two distinct MMAE strategies using either constant-gain or time-varying gain Kalman filters to identify the true model of the MSD system. Assuming that the true MSD model belongs to the set of models adopted, simulation results of the constant-gain and time-varying gain MMAE algorithms (under a variety of different sensor configurations, measurement noise, and mass uncertainties) show that both MMAE algorithms identify the true model of the MSD system and are robust to uncertainties. Furthermore, identification achieved by time-varying gain MMAE algorithms shows a slight improvement over constant-gain MMAE algorithms.** [1]

***Index Terms*— Multiple-Model Adaptive Estimation, Kalman filtering, System Identification and Modeling**

I. Introduction

Mass-Spring-Dashpot (MSD) systems arise in many applications in industrial and manufacturing systems, automotive active suspensions, flexible manipulators, and space structures to name but a few. Many works dealing with estimation and identification problems in such applications have been carried out. There is, however, a growing need to develop fast-robust estimators under parameter uncertainties. Most estimation algorithms, such as the Kalman Filter (see e.g., [1], [2]), are based on the nominal system model. However, in many cases, there are uncertainties in model parameters and even model structures. Estimators, which are designed without taking into account parameter uncertainties, may perform quite poorly in such applications. This problem has been addressed in the literature in the scope of robust estimator designing with performance-robustness in the presence of model uncertainties. The so-called multiple-model adaptive estimation (MMAE) methodology is a model-based adaptive estimation strategy using a set of models rather than insisting a single model (see, e.g. [1]-[3]). The MMAE can be used to handle parametric uncertainties and hence has become popular for many applications (see, e.g., [4]-[7]). In this paper, MMAE algorithms using either constant or time-varying gain Kalman filters as well as steady-state or time-varying residual covariance matrices are evaluated for identification of a complex MSD system in the presence of uncertain masses. Each mass in any configuration of the MSD system has a specific nominal value, but is considered uncertain and can vary between known limits. The MSD system is drived by the deterministic control forces. There are external disturbances on the masses and measurement noise on the sensors under Gaussian assumptions. We assume that the true MSD system belongs to set of N models designed in the architecture of the MMAE. In Sections II and III, the Kalman filter and the MMAE algorithm are discussed briefly. In Section IV, the dynamical MSD system is introduced. Simulation results are shown for both seady-state gain and time-varying gain MMAE algorithms under different noisy measurement assumptions in Section V. Concluding remarks and discussion about performance evaluation of the MMAE identification strategies are summarized in Section VI.

[1]This work was supported in part by a PhD grant from the FCT (Portuguese Foundation for Science and Technology) under program Ref. SFRH/BD/6199/2001.

II. Discrete-Time Kalman Filtering

The Kalman filtering (KF) algorithm, perhaps, is the best-known estimation method for linear systems where its important (and desirable) property is that it converges when the system is stable and time-invarient [1]. It can be implemented in the linear continuous-time or discrete-time systems based on the Bayesian state estimation. For the sake of using MMAE methodology, the discrete-time version KF has been used in this study.

Consider the kth model of a dynamical system

$$x_k(t+1) = A_k x_k(t) + B_k u(t) + L_k \xi(t) \quad (1)$$

$$z_k(t+1) = C_k x_k(t+1) + \theta(t+1) \quad (2)$$

where $x_k(t) \in \mathcal{R}^n$ is the state vector of the kth model at time t, $u_k(t) \in \mathcal{R}^m$ is the control input (which in mechanical systems is the various actuators), $z_k(t) \in \mathcal{R}^r$ is the noisy measurement vector, $\xi(t) \in \mathcal{R}^p$ is white noise process and $\theta(t) \in \mathcal{R}^r$ is measurement noise.

The fundamental problem associated with such a linear system is to compute the best estimate of the state $x(t)$ from the noisy measurements $\{z(\tau); 0 \leq \tau \leq t\}$ using a discrete KF, which is driven by the control vector $u(t)$ as well as the noisy measured output. The KF based on kth model generates a state estimate vector $\hat{x}_k(t)$ and an output estimate vector $\hat{z}_k(t+1|t)$ as shown in Fig. 1.

The recursive KF algorithm minimizes the covariance of the estimation error using two cycles, *prediction cycle* that propagates the state mean using a model of system dynamics and *update cycle* that updates the predicted mean with measurement information. The prediction and update cycles are repeated for each available measurement. The solution of KF for the kth model, utilizing these two cycles, is provided below.

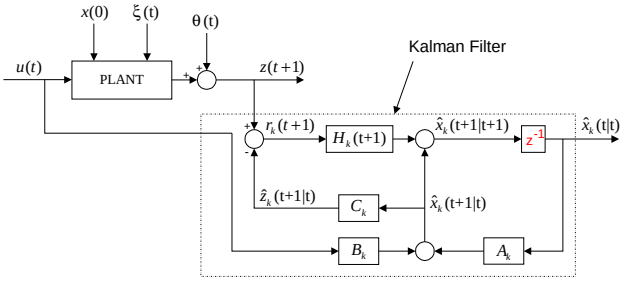

Fig. 1. The discrete-time Kalman filter

***Prediction cycle*: The predicted state covariance matrix $\Sigma_k(t+1|t)$ together with the predicted state estimate $\hat{x}_k(t+1|t)$ at time $t+1$, are computed as**

$$\hat{x}_k(t+1|t) = A_k\hat{x}_k(t|t) + B_k u(t) \quad (3)$$

$$\Sigma_k(t+1|t) = A_k\Sigma_k(t|t)A_k^T + L_k\Xi_k L_k^T \quad (4)$$

where $\Sigma_k(t|t)$ is the updated state covariance matrix at time t with the given state covariance of the kth model at time 0, $\Sigma_{k0} = \Sigma_k(0|0)$, and Ξ is the intensity matrix of the white noise process. *Update cycle*: The updated state estimate $\hat{x}_k(t+1|t+1)$ and the updated error covariance matrix $\Sigma_k(t+1|t+1)$ at time $t+1$ are defined in (5) and (6), respectively.

$$\hat{x}_k(t+1|t+1) = \hat{x}_k(t+1|t) + H_k[z_k(t+1) - C_k\hat{x}_k(t+1|t)] \quad (5)$$

$$\Sigma_k(t+1|t+1) = \Sigma_k(t+1|t). [I - C_k^T S_k^{-1}(t+1)C_k\Sigma_k(t+1|t)] \quad (6)$$

The so-called residual covariance matrix of the kth model at time $t+1$ is defined as

$$S_k(t+1) = cov[r_k(t+1); r_k(\tau+1)] = C_k\Sigma_k(t+1|t)C_k^T + \Theta \quad (7)$$

where Θ is intensity matrix of the measurement white noise. The KF gain matrix of the kth model, $H_k(t) \in \mathcal{R}^{n\times r}$, is defined as

$$H_k(t) = \Sigma_k(t+1|t+1)C_k^T\Theta^{-1} \quad (8)$$

The residual vector of the kth model at time $t+1$ is

$$r_k(t+1) = z(t+1) - \hat{z}_k(t+1|t) \quad (9)$$

which is depicted in Fig. 1.

III. Multiple-Model Adaptive Estimation (MMAE) Algorithm

The Multiple-Model Adaptive Estimation (MMAE) filter architecture is shown in Fig. 2 where the unknown plant can be a linear time-varying system with the stochastic inputs. The dynamical model of the plant is assumed to belong in the given model set.

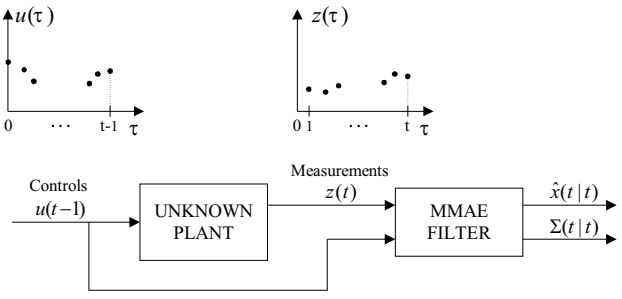

Fig. 2. Visualization of the MMAE Filter

Let us assume the set of past controls and measurements to be $Z(t) = \{u(0), u(1), u(2), \ldots, u(t-1), z(1), z(2), \ldots, z(t)\}$. This vector drives the MMAE filter to generate both the updated state estimate $\hat{x}(t|t)$ and the state covariance matrix $\Sigma(t|t)$ of the present state vector $x(t)$ using (10)-(11). respectively.

$$\hat{x}(t|t) = E\{x(t)|Z(t)\} \quad (10)$$

$$\Sigma(t|t) = E\{[x(t) - \hat{x}(t|t)][x(t) - \hat{x}(t|t)]^T|Z(t)\} \quad (11)$$

The equations (10)-(11) show that the MMAE filter updates the state estimate and covariance matrix at any time a new control is applied or a new sensor measurement is obtained.

The objective of developing the MMAE architecture is to identify an unknown linear system and estimate its state variables. In the MMAE algorithm, as shown in Fig. 3, we construct a bank of N parallel Kalman filters. Each KF is being matched to the corresponding model. Assume that the unknown system is one of the N known linear systems, but we do not know at the initial time t=0 which one. Thus, at time t=0 each one of the N models has the same initial probability of being the true one. Each KF is driven by the same deterministic control applied to the unknown system as well as by the noisy measurements generated by the unknown system. Then each KF generates a local state estimate and a residual signal, together with state-covariance and residual-covariance matrices, see (5)- (9). It is then possible to evaluate in real time the *posterior probability*, $P_i(t)$, that each of the N models is indeed the unknown system, given the measurements up to time t. The optimal state estimate is obtained by weighting the individual Kalman filter state-estimates by the respective posterior probabilities. We can also calculate the correct (global) state-covariance matrix on-line. The theory guarantees that as we obtain more and more measurements, the unknown system will be identified with probability one, see e.g., [3]. All of the N available KF residual vectors are used to generate (on-line) the posterior probabilities for $t = 1, 2, \ldots, \infty$, defined as

$$P_k(t) = Prob\{\textbf{kth model is true model}|Z(t)\} \quad \forall k = 1, 2, \ldots, N.$$

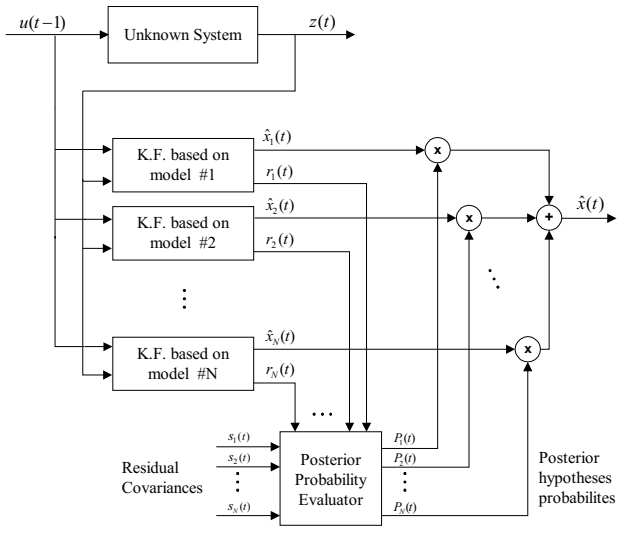

Fig. 3. The architecture of the MMAE Filter structure

It has been shown that maximum likelihood and related Bayesian identification procedures converge to a model in the model set, which is closest to the actual system generating the observations in the information distance measure even if the model set under consideration does not necessarily include the observed system [8]-[9]. We have consequently assumed that the true model is included in the given model set in studying of identification and modeling results.

The initial probabilities called *prior probabilities* are assumed to be given as $P_k(0)$, such that $\Sigma_{k=0}^{N} P_k(0) = 1$ and $P_k(0) \geq 0$ for all $k = 1, 2, \ldots, N$. The dynamics of the posterior probability evaluator, as a probability weighting computation unit, are shown in (12)-(14) in which the prior probabilities $P_k(0)$ are known and $r_k(t)$ and $S_k(t)$ are the residual vector and the covariance matrix of the kth Kalman filter, respectively. See (7)-(9).

$$P_k(t+1) = \frac{\beta_k(t+1)e^{-\frac{1}{2}w_k(t+1)}}{\sum_{j=1}^{N}\beta_j(t+1)e^{-\frac{1}{2}w_j(t+1)}P_j(t)}P_k(t) \quad (12)$$

$$\beta_k(t+1) = \frac{1}{(2\pi)^{m/2}\det S_k(t+1)^{1/2}} \quad (13)$$

$$w_k(t+1) = r_k^T(t+1)S_k^{-1}(t+1)r_k(t+1) \quad (14)$$

After computing all posterior probabilities $P_k(t)$ for all hypotheses (models) at time t, the state estimate and the state covariance matrix are computed as

$$\hat{x}(t|t) = \sum_{k=1}^{N} P_k(t)\hat{x}_k(t|t) \quad (15)$$

$$\Sigma(t|t) = \sum_{k=1}^{N} P_k(t). \left[\Sigma_k(t|t) + [\hat{x}_k(t|t) - \hat{x}(t|t)]\,[\hat{x}_k(t|t) - \hat{x}(t|t)]^T\right] \quad (16)$$

It should be noticed, (see [1], [3]), that the time-varying gain MMAE is a truly optimal estimator, in the sense that it computes the conditional mean and covariance of the state, under Gaussian assumptions. The *suboptimal* constant-gain MMAE algorithm uses steady-state KF, in the sense that each KF gain, $H_k(t)$, in Eq. (8) is replaced by its constant steady-state value, H_k. Also, the residual covariance matrices, $S_k(t)$, in Eq. (7) are also replaced by their constant steady-state values, S_k, and used in the posterior probability evaluation of Eq. (12).

IV. Dynamic model of the MSD system

As a case study, consider a continuous-time eighth order LTI mass-spring-dashpot system shown in Fig. 4. In this figure, x_i and x_{i+4} denote the position and velocity, respectively, of mass $M_i (i = 1, 2, 3, 4)$.

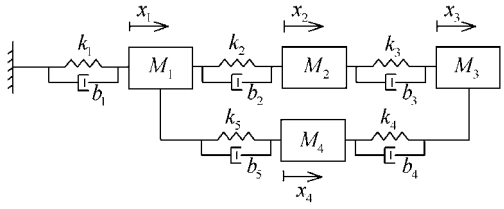

Fig. 4. The MSD system

Let us take the position and velocity of each mass as states to be $x(t) = [x_1\, x_2\, x_3\, x_4\, \dot{x}_1\, \dot{x}_2\, \dot{x}_3\, \dot{x}_4]^T$ (measuring from equilibrium). The continuous-time dynamics of the motion are

$$\dot{x}(t) = Ax(t) + Bu(t) + L\xi(t) \quad (17)$$

$$z(t) = Cx(t) + \theta(t) \quad (18)$$

where $A, B, C,$ and L are continuous-time state matrix, input matrix, output matrix and process noise gain matrix, respectively as follow.

$$A = \begin{bmatrix} \mathbf{0}_{4\times4} & \mathbf{I}_{4\times4} \\ A_{21} & A_{22} \end{bmatrix}$$

$$A_{21} = \begin{bmatrix} -\frac{(k_1+k_2+k_5)}{m_1} & \frac{k_2}{m_1} & 0 & \frac{k_5}{m_1} \\ \frac{k_2}{m_2} & -\frac{(k_2+k_3)}{m_2} & \frac{k_3}{m_2} & 0 \\ 0 & \frac{k_3}{m_3} & -\frac{(k_3+k_4)}{m_3} & \frac{k_4}{m_3} \\ \frac{k_5}{m_4} & 0 & \frac{k_4}{m_4} & -\frac{(k_4+k_5)}{m_4} \end{bmatrix}$$

$$A_{22} = \begin{bmatrix} -\frac{(b_1+b_2+b_5)}{m_1} & \frac{b_2}{m_1} & 0 & \frac{b_5}{m_1} \\ \frac{b_2}{m_2} & -\frac{(b_2+b_3)}{m_2} & \frac{b_3}{m_2} & 0 \\ 0 & \frac{b_3}{m_3} & -\frac{(b_3+b_4)}{m_3} & \frac{b_4}{m_3} \\ \frac{b_5}{m_4} & 0 & \frac{b_4}{m_4} & -\frac{(b_4+b_5)}{m_4} \end{bmatrix}$$

$$B = \begin{bmatrix} \mathbf{0}_{4\times4} \\ B_{21} \end{bmatrix}; B_{21} = diag(1/m_i); L = \begin{bmatrix} \mathbf{0}_{4\times4} \\ L_{21} \end{bmatrix}; L_{21} = diag(l_i/m_i)$$

$$C = \begin{cases} [\,0\;0\;1\;\mathbf{0}_{1\times5}\,]; & \textbf{one position measurement } (z_3) \\ \left[\begin{smallmatrix} 1&0&0&\mathbf{0}_{1\times5} \\ 0&0&1&\mathbf{0}_{1\times5} \end{smallmatrix}\right]; & \textbf{two position measurements } (z_1 \textbf{ and } z_3) \\ [\,\mathbf{I}_{4\times4}\;\mathbf{0}_{4\times4}\,]; & \textbf{four position measurements } (z_1, \ldots, z_4) \end{cases} \quad (19)$$

The equations above indicate that we have treated the external force u as the control input. There are, however, external forces (plant disturbances) that affect the system and act despite our will. It should also be emphasized that we shall discretize the continuous-time MSD system together with all the models to obtain the correspondent discrete models so as to apply the discrete-time MMAE methodology. $[A_k, L_k]$ and $[A_k, C_k]$ are assumed stabilizable and detectable for all models, respectively.

V. Simulation results

We evaluate the system in three different sensor combinations i.e. one, two and four measurements. For the one measurement case, the only sensor in the system measures the displacement of the third mass alone. There is noise in this sensor. Similarly, for the two measurement case, the displacements of the first and third masses and for four measurement case, all displacements of all masses are measured. The average of 100 Monte-Carlo simulation results are provided for both constant-gain and time-varying gain MMAE algorithms. The statistical assumptions below have been used in our results.

- **The measurement noise $\theta(t)$ is a stationary white noise (sensor noise) with intensity matrix Θ.**
- **The process noise $\xi(t)$ is a stationary white noise with intensity matrix Ξ.**
- **$\xi(t)$ and $\theta(t)$ are Gaussian, independent and there is no correlation between them, $cov[\xi(t); \theta(\tau)] = 0$.**
- **The initial state vector $x(0)$ is a Gaussian random variable with zero mean and covariance $cov[x(0); x(0)] = \Sigma_0$. It is also assumed to be uncorrelated with all noises.**

The nominal parameters of the MSD system (mass, damper and spring stiffness coefficients) are assumed linear and time-invariant. Their values convey natural frequencies less than $\omega = 10rad/sec$ and damping ratios $\zeta \leq 0.01$ showing that the system is a lightly-damped MSD system. Table I shows the mass coefficients of the true system and four different models used in MMAE algorithms. The mass parameter set $\mathcal{M}_i \in \mathbb{R}^+$ is a closed interval $\mathcal{M}_i = \{m_i : m_i^{min} \leq m_i \leq m_i^{max}\}$. For example, the true M_2 is an unit mass for which the discrete mass model set is $\mathcal{M}_2 = \{0.5, 1, 2, 3\}$. For the rest of masses, uncertainties are taken as $0.5 \leq M_1 \leq 3.0$, $0.5 \leq M_2 \leq 3.0$, $0.2 \leq M_3 \leq 2.0$ and $0.5 \leq M_4 \leq 3.0$ whereas their true values are 2, 1, 0.5 and 1, respectively. Also, note that model #1 is always the correct model of the MSD system.

Fig. 5 shows the control force F_u and F_c applied on the unknown mass and the mass M_4, respectively. It is also assumed that F_c drives the mass M_2 when mass M_4 is uncertain. The other parameters used in the simulations are listed below.

- **Spring stiffness coefficients of the MSD system and all the models: $k = 10 (i = 1, .., 5)$**
- **Damping coefficients of the MSD system and all the models: $b_i = 0.01 (i = 1, .., 5)$**
- **Sampling time of simulations: $T_s = 10msec$ (to translate it into a discrete-time LTI system)**
- **Prior probabilities: $P_k(0) = 0.25\ \forall k = 1, 2, 3, 4$**
- **Initial state vector of true system and all the models: $x(0) = [0]_{8\times1}$**
- **Covariance of the initial state: $E\{x_0(t)x_0^T(\tau)\} = \Sigma_0 = diag(0.1)$**
- **Intensity of the process noise: $\Xi = diag(1)$**
- **Low measurement noise intensity: $\Theta_L = diag(0.01)$**

TABLE I

THE MASS COEFFICIENTS OF ALL MODELS

Uncertain mass	MSD system	m_1	m_2	m_3	m_4
M_1	Model #1 (True)	2.00	1.00	0.50	1.00
	Model #2	0.50	1.00	0.50	1.00
	Model #3	1.00	1.00	0.50	1.00
	Model #4	3.00	1.00	0.50	1.00
M_2	Model #1(True)	2.00	1.00	0.50	1.00
	Model #2	2.00	0.50	0.50	1.00
	Model #3	2.00	2.00	0.50	1.00
	Model #4	2.00	3.00	0.50	1.00
M_3	Model #1(True)	2.00	1.00	0.50	1.00
	Model #2	2.00	1.00	0.200	1.00
	Model #3	2.00	1.00	1.000	1.00
	Model #4	2.00	1.00	2.00	1.00
M_4	Model #1(True)	2.00	1.00	0.50	1.00
	Model #2	2.00	1.00	0.50	0.50
	Model #3	2.00	1.00	0.50	2.00
	Model #4	2.00	1.00	0.50	3.00

- **High measurement noise intensity:** $\Theta_H = diag(1.0)$
- **Elements inserted in the matrix gain** L_{21} **of the white noise process:** $l_i = 10$**, see** (19)**.**

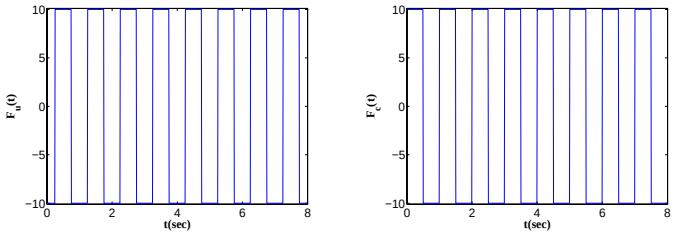

(a) Exerted force on uncertain mass (b) Exerted force on the known mass

Fig. 5. Driving forces used in the MSD and all models. $F_u(t)$ **and** $F_c(t)$ **are exerted on uncertain mass and the mass** M_4**, respectively.** $F_c(t)$ **drives the mass** M_2 **when the mass** M_4 **is uncertain.**

Figs. 6-7 show the performance evaluation of the constant-gain MMAE algorithms for three different measurement configurations i.e. using one displacement measurement of mass M_3 **(case 1), two displacement measurements of masses** M_1 **and** M_3 **(case 2) and all displacement measurements of all masses (case 3). As it can be seen from all simulation results, the posterior probability of model #1,** $P_1(t)$**, reaches unity eventually (as it is expected) certifying that MMAE algorithms recognize the correct model. Furthermore, the identification and modeling results under the influence of low intensity measurement noise are faster than those with high intensity measurement noise. Figs. 6(a)-7(a) depict the posterior probability results associated with uncertain mass** M_1 **for all measurement cases. The displacement of the uncertain mass** M_1 **is measured in both case 2 and case 3 and hence these two cases identify the correct model, approximately at the same time, faster than the case 1.**

Figs. 6(b)-7(b) present the posterior probability results associated with uncertain mass M_2 **for all measurement cases. Since there is no measurement on mass** M_2 **in case 1 and case 2, the case 3 identifies the correct model faster than those cases. In fact, while all measurement cases identify the correct model, identification of constant-gain MMAE algorithm with four sensors is faster than other measurement configurations since it has a measurement on uncertain mass. However, the identification process in case 3 is faster only due to using the displacement sensor on mass** M_2**.**

Figs. 6(c)-7(c) show the posterior probability results with uncertain mass M_3**. As shown, since the displacement of the uncertain mass** M_3 **is measured in all cases, the achieved identification yields almost equal results. Therefore, putting additional sensors on the other certain masses seem fruitless as long as the displacement of the uncertain mass is measured.**

The identification results of the MMAE with uncertain mass M_4 **are depicted in Figs. 6(d)-7(d) where case 1 and case 2 identify the correct model closely. However, case 3 (which contains a measurement on uncertain mass** M_4 **is faster than the cases 1 and 2.**

The posterior probability of the model #1, $P_1(t)$**, using time-varying gain MMAE algorithms are shown in Figs. 8-9. Three different measurement configurations are the same we used in constant-gain MMAE algorithms. Similarly, under the influence of low measurement noise, time-varying gain MMAE algorithms are able to identify the true model faster than that of high measurement noise. One can see that parameter identification results of the MSD system are similar to that of the constant-gain MMAE algorithms. However, due to using the time-varying KF gains as well as the time-varying residual covariance matrices in time-varying gain MMAE algorithms, identification process achieved by time-varying algorithms are better than the constant-gain MMAE algorithms. Also, similar to constant-gain results, there is a noticeable time difference between system identification in case 1, case 2 and case 3 measurement configurations with uncertain mass** M_2 **or mass** M_4**, as shown in Figs. 8(b)-9(b) and Figs. 8(d)-9(d), respectively. It is also seen that using additional sensors in measurement configuration in Figs. 8(c)-9(c), with an uncertain mass** M_3**, does not improve the filter performance. However, significant improvement is obvious in other cases.**

In conclusion, if there is no measurement on the uncertain mass, although the true model can be identified properly, the identification process is considerably slow. Using either MMAE algorithm, the more displacement sensor approaches an uncertain mass, the better identification results are gained which somehow makes intuitive sense! Thus, putting the sensors on the uncertain masses to measure their displacements in the MMAE algorithms is more informative rather putting on the known ones.

VI. CONCLUSION

In this paper, we presented the performance evaluation of two multiple-model adaptive estimation algorithms for identification and modeling of a complex mass-spring-dashpot system in the face of the mass uncertainties. Simulation results illustrated that both constant-gain and time-varying gain MMAE filters yield acceptable identification results in this MSD system with mass uncertainties. The results obtained by the time-varying MMAE methodology do not show significant improvement over that of the constant-gain MMAE. Since constant-gain MMAE algorithms are computationally much simpler, it is conjectured that they can be used with confidence in other applications. Meanwhile, advances in computational speed and digital parallel computer hardware and software make MMAE-type of implementations more and more practical for very complex identification and state estimation problems constructing more linear models within the model set under consideration. Doing so, the MMAE algorithms would be a better solution for identifying and modeling the actual-unknown plant perfectly among the provided model set.

REFERENCES

[1] B. Anderson and J. Moore, ***Optimal Filtering*****, Prentice Hall, Englewood cliffs, 1979.**

[2] P. S. Maybeck, ***Stochastic Models, Estimation and Control*****, Vol. 1, Navtech Press, Arlington, Virginia, 1994.**

[3] M. Athans and C. B. Chang, "Adaptive estimation and parameter identification using multiple model estimation algorithms", Technical note 1976-28, MIT Lincoln lab., Lexington, MA, June 1976.

[4] K. D. Schott and B. W. Bequette, "Multiple Model Adaptive Control", In ***Multiple Model Approaches to Modelling and Control*****, R. Murray-Smith and T. A. Johnsen (eds.), Chapter 11, pp. 269–292, Taylor & Francis, UK, 1997.**

[5] M. Athans et al, "The stochastic control of the F-8C aircraft using the multiple model adaptive control (MMAC) method - Part I: equilibrium flight", IEEE Trans. on Automatic Control, Vol. 22, No. 5, pp. 768–780, Oct. 1977.

[6] G. Schiller and P. S. Maybeck, "Control of a large space structure using MMAE/MMAC techniques", IEEE Trans. on Aerospace and Electronic Systems, Vol. 33, No. 4, pp. 1122–1130, Oct. 1997.

[7] Y. Oshman et al, "Using a Multiple Model Adaptive Estimator in a Random Evasion Missile/Aircraft Encounter", Journal of Guidance, Control and Dynamics, Vol. 24, No. 6, pp. 1176–1186, Nov.-Dec. 2001.

[8] Y. Baram and Nils. R Sandell, "An information Theoretic approach to dynamical systems modeling and identification", IEEE Trans. on Automatic Control, Vol. 23, No. 1, pp. 61–66, Feb. 1978.

[9] Y. Baram and Nils. R Sandell, "Consistent estimation on finite parameter sets with application to linear systems identification", IEEE Trans. on Automatic Control, Vol. 23, pp. 451–454 , June 1978.

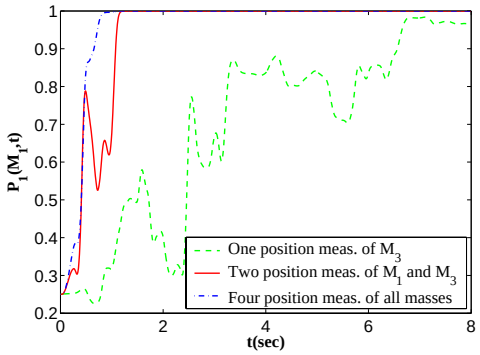

(a) Uncertainty in mass M_1

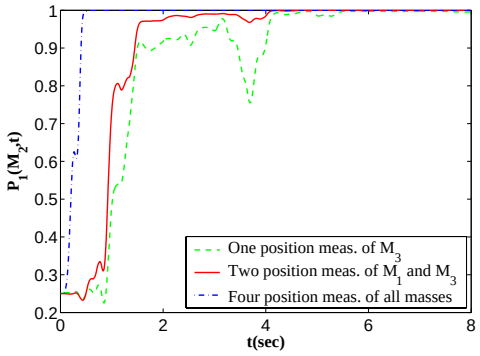

(b) Uncertainty in mass M_2

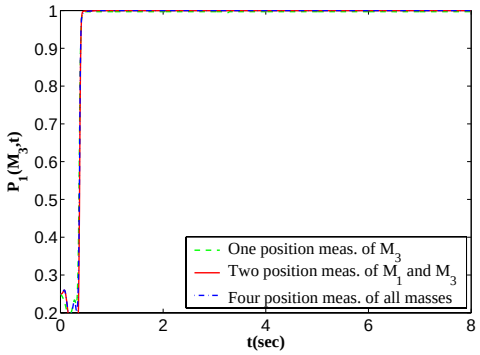

(c) Uncertainty in mass M_3

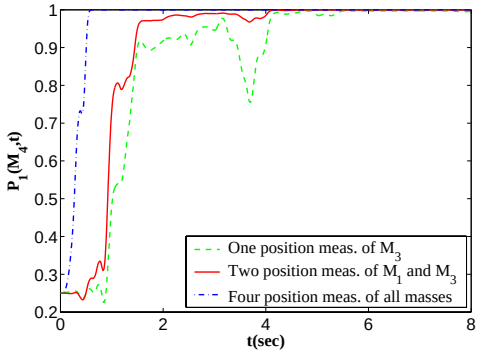

(d) Uncertainty in mass M_4

Fig. 6. The posterior probabilities of the true model (#1) using *constant-gain MMAE under low intensity measurement noise*

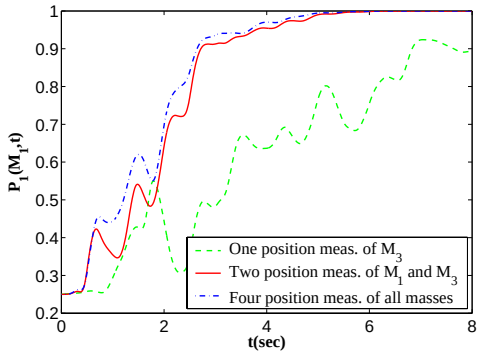

(a) Uncertainty in mass M_1

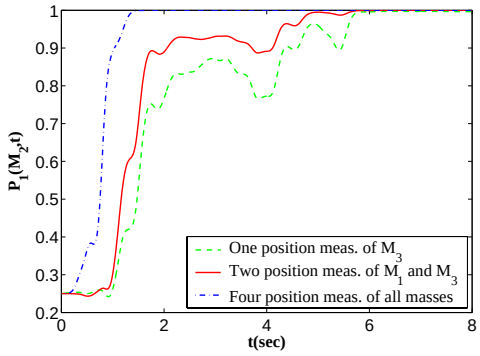

(b) Uncertainty in mass M_2

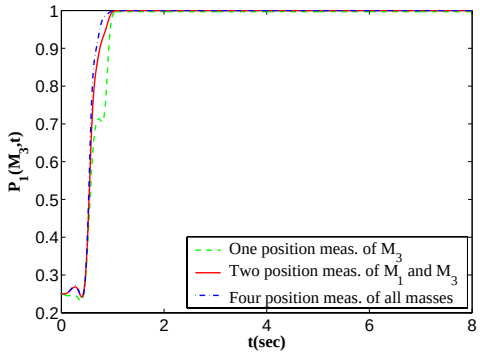

(c) Uncertainty in mass M_3

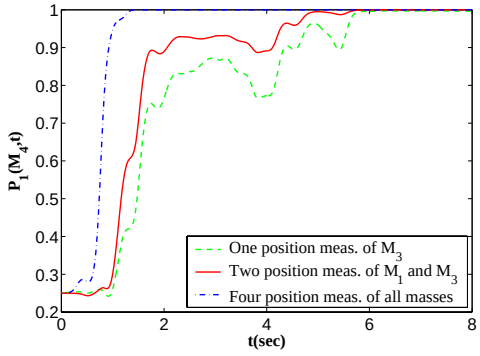

(d) Uncertainty in mass M_4

Fig. 7. The posterior probabilities of the true model (#1) using *constant-gain MMAE under high intensity measurement noise*

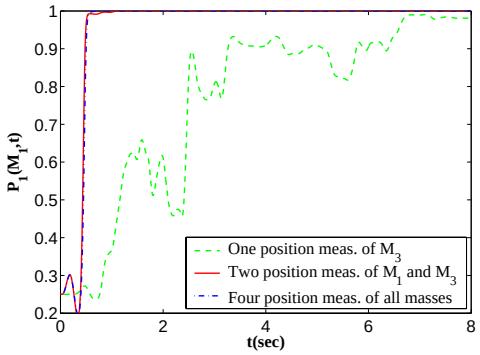

(a) Uncertainty in mass M_1

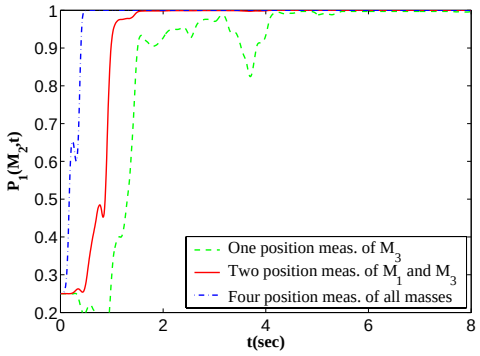

(b) Uncertainty in mass M_2

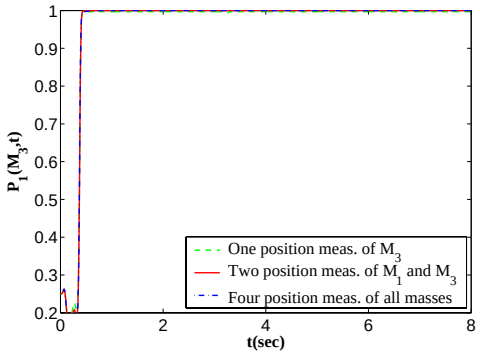

(c) Uncertainty in mass M_3

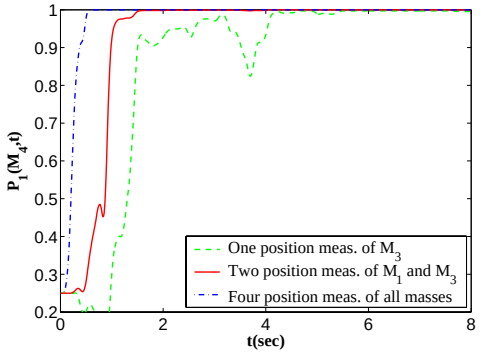

(d) Uncertainty in mass M_4

Fig. 8. The posterior probabilities of the true model (#1) using *time-varying-gain MMAE under low intensity measurement noise*

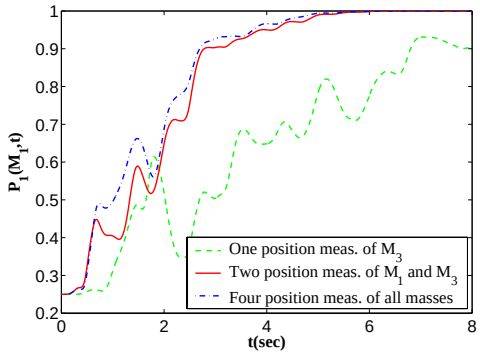

(a) Uncertainty in mass M_1

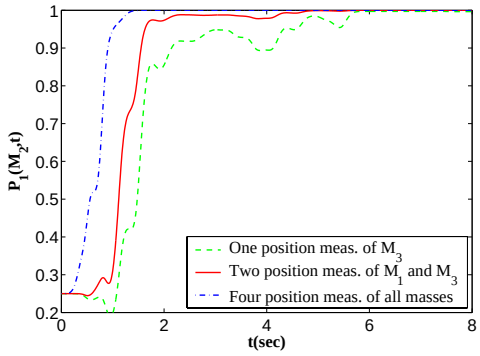

(b) Uncertainty in mass M_2

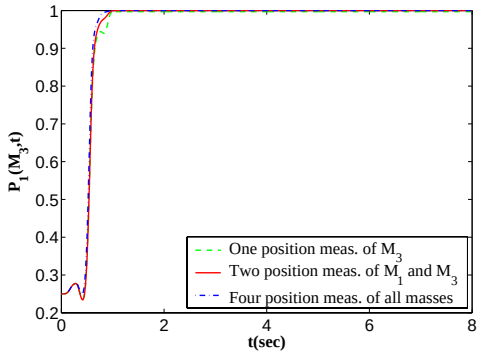

(c) Uncertainty in mass M_3

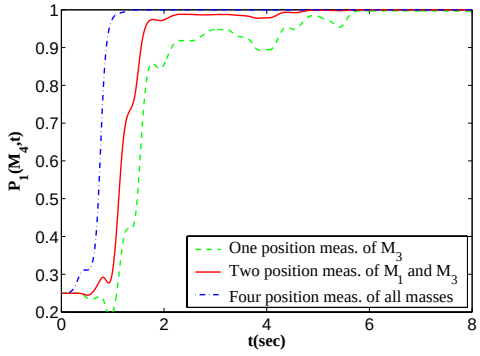

(d) Uncertainty in mass M_4

Fig. 9. The posterior probabilities of the true model (#1) using *time-varying-gain MMAE under high intensity measurement noise*